Design of an E-band Self-Biased Field-Displacement Isolator using Al-doped Strontium Hexaferrite for SATCOM applications

Evan Roué, Vincent Laur, Antoine Hoez, Alexis Chevalier, Jean-Luc Mattei, Gérard Tanné, Olivier Vendier, Rose-Marie Sauvage

Design of an E-band Self-Biased Field-Displacement Isolator using Al-doped Strontium Hexaferrite for SATCOM applications

Evan Roué[(1)], Vincent Laur[(1)], Antoine Hoez[(1)], Alexis Chevalier[(1)], Jean-Luc Mattei[(1)], Gérard Tanné[(1)], Olivier Vendier[(2)], Rose-Marie Sauvage[(3)]

[(1)]Lab-STICC, UMR 6285, CNRS, Université de Bretagne Occidentale
6 Avenue Victor Le Gorgeu, 29200 Brest, France
Email: Evan.Roue@univ-brest.fr

[(2)] Thales Alenia Space
26 Avenue Jean François Champollion, 31100 Toulouse, France

[(3)] Agence de l'Innovation de Défense, Direction Générale de l'Armement
60 Boulevard du Général Martial Valin, CS 21623, 75509 Paris cedex 15, France

INTRODUCTION

SATCOM systems are used for broadcasting TV or internet around the world. Due to the generalization of video streaming and online gaming, the demand for high-speed satellite communications grows exponentially. Associated with the fast-growing amount of users, space service providers and satellite manufacturers are forced to expand the capacity of their systems, leading to more spectrum usage. Future feeder links will use the 71 – 76 GHz band for downlink and from 81 – 86 GHz for uplink. Because the free-space wavelength is small at these frequency bands, components design is challenging. Moreover, space systems now feature dynamic resource allocation. Using active electronically scanned arrays (AESAs), satellite operators can focus antenna beams on regions of the world that need most of the satellite throughput at a specific time. Huge amount of RF front-ends closely spaced are needed to build AESAs.

Isolators are usually used in space RF chains to decouple amplifiers and to mitigate active VSWR issues in AESAs. A solution based on a circulator and a termination cannot be used as the antenna spacing constraint is strong. Therefore, a strong need for cheap and small components that are completely contained in the cross section of a standard rectangular waveguide rises. Inline isolators such as resonance isolators or field-displacement isolators can fulfill the need. Traditionally, they use soft ferrites such as garnet or spinel. So, they require an external field created by permanent magnets, placed outside the waveguide, to work. It is possible to remove external magnets using hard ferrites, such as pre-oriented barium or strontium hexaferrites. Those devices are called self-biased devices. Self-biased ferrites devices are interesting for space application as they are small, lightweight and robust to external magnetic field.

In this work, we demonstrate the ability to create an E-band self-biased field-displacement isolator. In order to use the field-displacement effect at E-band, the hexaferrite should have a high anisotropy field of 25 kOe. Pure barium hexaferrites have an anisotropy field of around 18 kOe and their strontium counterparts are closer to 20 kOe. Thus, a custom hexaferrite is needed for the E-band self-biased isolator. Here, an aluminum-doped strontium hexaferrite is synthesized and characterized. Aluminum doping is well-known to enhance the anisotropy field [1].

For ease of manufacturing, fused deposition modelling (FDM) 3D-printing technique is used to create the resistive layer with a lossy dielectric material of carbon-loaded polylactic acid (PLA-C), based on previous work at the laboratory [2]. A dielectric spacer is also added, made out of polylactic acid (PLA), to accurately place the ferrite slab in the waveguide.

BASIC PRINCIPLES OF FIELD-DISPLACEMENT ISOLATORS

In a ferrite material, permeability becomes anisotropic in the presence of a magnetic field and should be modelled as a tensor. If the ferrite is saturated along the z-axis, we can use Polder's equations [3]:

$$[\mu_r] = \begin{bmatrix} \mu & j\kappa & 0 \\ -j\kappa & \mu & 0 \\ 0 & 0 & 1 \end{bmatrix} \tag{1}$$

$$\mu = 1 + \frac{(\omega_0 + j\alpha\omega)\omega_m}{(\omega_0 + j\alpha\omega)^2 - \omega^2}; \quad \kappa = \frac{\omega\omega_m}{(\omega_0 + j\alpha\omega)^2 - \omega^2}$$

$$\omega_0 = \gamma H_{int}; \quad \omega_m = \gamma 4\pi M_s; \quad \alpha = \frac{\gamma \Delta H_{mes}}{2\omega_{mes}}.$$

Here, $\gamma = 2.8\ MHz/Oe$ is the gyromagnetic ratio, $\omega = 2\pi f$ is the frequency of the incident wave, $4\pi M_s$is the saturation magnetization and ΔH_{mes} is the gyromagnetic linewidth measured at the ω_{mes} frequency. The internal magnetic field H_{int} can be expressed as

$$H_{int} = H_0 + H_k - N_z M_s, \tag{2}$$

where H_0 is the external applied DC magnetic field, H_k is the magneto-crystalline anisotropy field and N_z is the z-axis demagnetizing factor. In a ferrite slab magnetized perpendicularly to the $\vec{H}$-field direction of an incident wave, the effective permeability is defined as follows

$$\mu_{r_{eff}} = \frac{\mu^2 - \kappa^2}{\mu}. \tag{3}$$

When $\mu_{r_{eff}} < 0$, fields distribution inside a transversely-magnetized ferrite slab is very different for forward and reverse waves. This phenomenon is called field-displacement and it was first described in [4] and analyzed in detailed in [5]. It allows for the creation of isolators with higher bandwidths and lower biasing fields than their gyro-resonance based counterparts.

Waveguide field-displacement isolators consists of a ferrite slab with a resistive layer on one face (see Fig. 1), with well-defined dimensions, precisely placed into the waveguide in order to have a null amplitude of $\vec{E}$-field on the resistive layer when the electromagnetic wave is travelling in the forward direction and in order to have the maximum amplitude of the $\vec{E}$-field on the same face when the wave is travelling in the reverse direction. So, the resistive layer absorbs most of the wave in the reverse direction while it is completely transparent in the forward direction due to the null amplitude. A similar behavior can be observed in planar edge-guided isolators [6] that lies on the same effect. where the $\vec{E}$-field is maximum on one edge (dependent on the direction of propagation) and decays exponentially along the width of the line.

MAIN DESIGN CONSIDERATIONS FOR SELF-BIASED DEVICES

When designing self-biased devices, first consideration is about ferrite magnetic properties. We need a ferrite material that can keep its magnetization in the absence of external magnetic field ($H_a = 0$). A solution to this is to use hexaferrites which offer quite high remanent-to-saturation magnetization ratio ($\frac{M_r}{M_s} > 0.8$), a remanent magnetization of a few thousands Gauss and a high anisotropy field ($H_k \sim 18$ kOe) that enables their use in millimeter wave systems [7].

Second consideration is about the working frequency band. Field-displacement isolators works only when $\mu_{r_{eff}} < 0$ which implies

$$\sqrt{\omega_0(\omega_0 + \omega_m)} < \omega < \omega_0 + \omega_m. \tag{4}$$

In other words, field-displacement effect occurs above the resonance of effective permeability, in a frequency band only limited by the magnetization. So, we need to put this resonance frequency close to the lower edge of the frequency band of interest. As there is no external applied magnetic field in self-biased devices, the only way to control the resonance frequency is to change the value of the anisotropy field by adjusting the chemical composition of the hexaferrite. Therefore, design of a custom material is required.

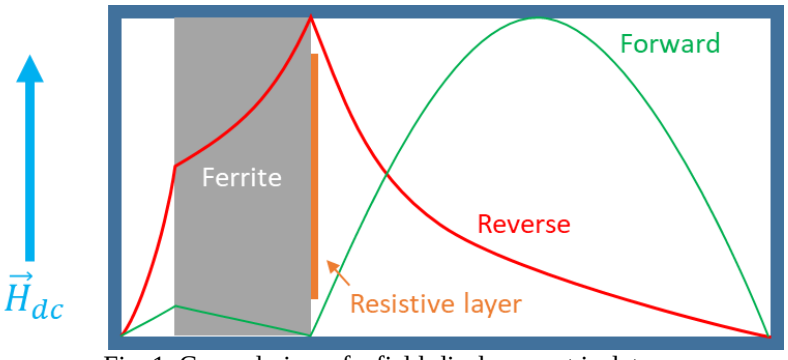

Fig. 1. General view of a field-displacement isolator.

Third consideration is impedance matching. Waves can be reflected at the input of the isolator instead of travelling through it if the average waveguide medium permittivity is too different from air ($\epsilon_r = 1$). Unfortunately, permittivity values of hexaferrites are quite high ($\epsilon_r \sim 20$). Thus, the ratio between the cross-section area of the ferrite slab and the cross-section area of the waveguide should be carefully controlled. A tradeoff has to be made between impedance matching and the reduction of the internal magnetic field due to demagnetizing factors.

DESIGN OF THE E-BAND SELF-BIASED FIELD-DISPLACEMENT ISOLATOR

Ferrite Material Synthesis and Characterization

In order to make an E-band (71 – 76 GHz) self-biased field-displacement isolator, we need a ferrite material that offers a $\mu_{r_{eff}}$ resonance frequency of around 70 GHz. This implies an anisotropy field H_k of around 25 kOe. According to [1], an anisotropy field of 23 kOe can be obtained with a substitution of x = 1 to $SrFe_{12-x}Al_xO_{19}$. By extrapolation of values they have obtained, an anisotropy field of 25 should be obtained for x = 1.6.

Al-doped strontium hexaferrites were made by a topotactical process developed at the laboratory [8], [9]. $SrFe_{10.4}Al_{1.6}O_{19}$ were fabricated with strontium carbonate $SrCO_3$ (Acros-organics®, Germany, 99%), goethite αFeO(OH) (made in laboratory) and aluminum oxide Al_2O_3 (Buehler®, USA, 99%). These components were mixed in the appropriate ratio with an agate mortar and the resulting mixture was pressed into parallelepiped pellet at a uniaxial pressure of 1.7 GPa. The pellet was then sintered at 1250 °C without dwelling time. Magnetic measurement was performed using a Vibrating Sample Magnetometer EZ9 from MicroSense® and Powder XRD analysis with a Panalytical® Empyrean® (Cu Kα radiation). Rietveld analysis was performed with Jana2020 [10]. The Rietveld analysis on the X-Ray diffraction pattern confirms the sample was monophasic $SrFe_{10.4}Al_{1.6}O_{19}$, the R-factors are referenced in Table 1. The sample exhibit a good M_r/M_s of 0.88 and a strong coercive field H_c of 8.525 kOe (Fig. 2. right). The magnetic properties of the material are listed in the Table 2.

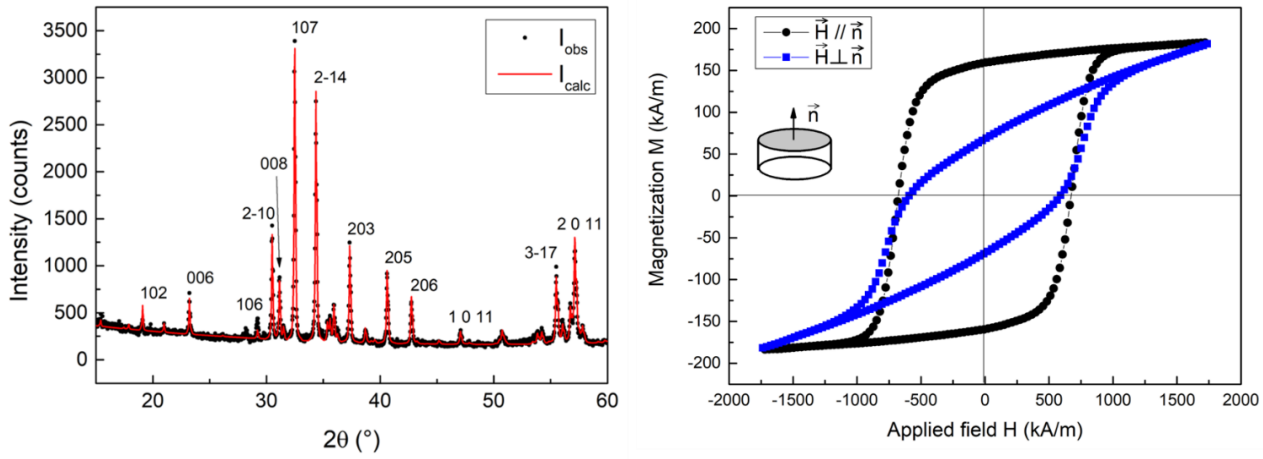

Fig. 2. Rietveld analysis on the powder diffraction pattern (left). Hysteresis cycle of the $SrFe_{10.4}Al_{1.6}O_{19}$ puck sample, with magnetizations along to $\vec{n}$ (circle) and perpendicular to $\vec{n}$ (square), respectively.

Table 1. Crystallographic data and Rietveld refinement

Crystallographic data	Space group	*a*, *c* (Å)	R_{obs}, R_{all}, GOF
ICSD 184962	*P*63/*mmc*	5.8523(3), 22.9389(14)	6.38, 8.49, 1.51

Table 2. Magnetic properties of the sample

Composition	Density (g/cm³)	$4\pi Ms\ (G)$	M_r/M_s	$H_c\ (Oe)$	$H_k\ (kOe)$
$SrFe_{10.4}Al_{1.6}O_{19}$	4.3	2274.5	0.88	8525	23 - 25

RF Design of the Component and EM Simulations

As the placement of the ferrite slab is critical to RF performance in field-displacement isolators and could be quite challenging at millimeter waves due to the small size of the waveguide, we chose to add a dielectric spacer. For ease of manufacturing, we decided to use a Fused Deposition Modelling (FDM) 3D-printer to shape this dielectric spacer out of polylactic acid (PLA). Its dielectric properties has already been determined using the same setup as [2]. Between 70 – 110 GHz, its permittivity and its dielectric loss tangent was found to be 2.4 and 0.02, respectively, regardless of the filament deposition direction. Based on previous work [2], [11], [12], we know that a carbon-loaded polylactic acid (PLA) filament can act as an RF absorber. Deposed in thin layers [12], this material can replace the expensive and cumbersome process of thin-film deposition of resistive layers. Thus, carbon-loaded PLA (called PLA-C) is used as the resistive layer of the field-displacement isolator. Here, relative permittivity of PLA-C is about 11 and dielectric loss tangent is about 0.4 at 70 – 110 GHz [2]. The final isolator design is shown on Fig. 3. The dielectric spacer extends longitudinally (1 mm on each side) to help supporting ferrite slabs and resistive layers. It also contributes to ensure a smooth transition between air and the ferrite.

EM simulations were done using Ansys® HFSS® to determine RF performance. Without direct measurement of the ferrite dielectric properties, an assumption has to be done in the simulation. Based on values found in commercial hexaferrite datasheets, the ferrite dielectric constant design value is set to 18 and the ferrite loss tangent design value is set to 5.10^{-4}. An optimization of the ferrite slab dimensions and the ferrite-to-wall spacing has been run to get low insertion loss and moderate isolation (criteria: $S_{21} > -0.7\ dB$ and $S_{12} < -12\ dB$) between 71 GHz and 76 GHz. Aharoni's equations for demagnetizing factors [13] are taken into account in the simulations. Ferrite slab final dimensions are 0.4 mm width, 0.4 mm tall and 11 mm long, so the z-axis demagnetizing factor is $N_z = 0.492$. Optimized PLA-C layer thickness is 0.2 mm. The ferrite-to-wall optimized spacing was found to be 0.1 mm. Simulated results are shown on Fig. 4. Maximum isolation level is 64.7 dB at 72.7 GHz and minimum insertion loss is 1.45 dB at 72.1 GHz. In the frequency band of interest (71 – 76 GHz), insertion loss is lower than 3.19 dB and isolation level is better than 12.2 dB. Return losses are higher than 25 dB between 67 GHz and 90 GHz and higher than 30 dB in the 71 GHz – 76 GHz range.

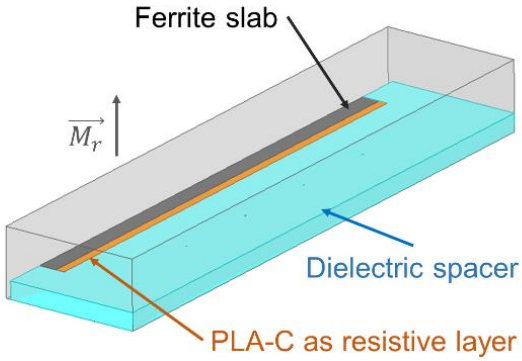

Fig. 3. 3D view of the E-band self-biased field-displacement isolator simulated design.

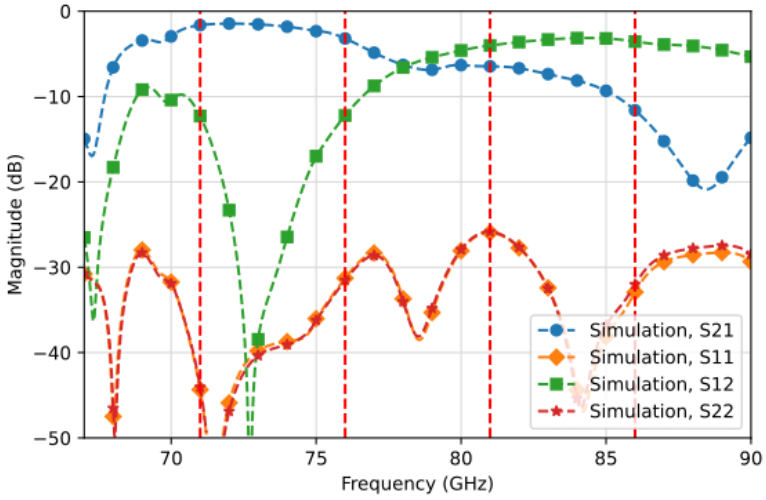

Fig. 4. Simulated S-parameters of the designed isolator. Red lines delimit E-band space communication frequency bands (71 – 76 GHz and 81 – 86 GHz).

REALIZATION OF THE E-BAND SELF-BIASED FIELD-DISPLACEMENT ISOLATOR

Once the final dimensions are known, the isolator is manufactured. The plastic part is 3D-printed using a Raise3D® Pro3® 3D printer. Hotend and bed temperatures are set to their default values in the slicer software ($T_{hotend} = 205°C, T_{bed} = 55°C$). Printer layer thickness is set to $100\ \mu m$. During the print time, the previously made ferrite slab is sanded and polished manually into the final dimensions ($0.4\ mm \times 0.4\ mm \times 11\ mm$). It is then glued to the 3D printed part to create the "insert" (see Fig. 5). The insert is placed into a $1\ inch$-long ($25.4\ mm$) WR-12 waveguide.

The component has been measured using Rohde & Schwartz® ZVA67 vector network analyzer with ZVA-110 W-band (75 – 110 GHz) frequency converters. WR-10 to WR-12 waveguide transitions are added to fit the component onto the converters and onto the termination. A Thru-Reflect-Line (TRL) calibration is done with WR-10 waveguide calibration kit due to the lack of WR-12 waveguide calibration kit. Thus, presented values are "as-measured" without de-embedding. In addition, transitions are measured back-to-back. The obtained insertion loss value is 0.4 dB. Frequency sweep is set from 67 GHz to 90 GHz with 1601 points, which is partially outside the recommended frequency band of the calibration kit (75 – 110 GHz). Measurement uncertainties are expected between 67 GHz to 75 GHz. Comparison between simulated and measured S-parameters are shown in Fig. 7.

The realized isolator maximum isolation level is 47 dB at 79.6 GHz with an insertion loss of 5.04 dB. Between 76.7 GHz and 82.3 GHz, isolation is better than 12 dB which means a relative bandwidth of 7%. Insertion loss stay around 5 dB on the whole frequency band of isolation ($S_{21} < -12\ dB$).

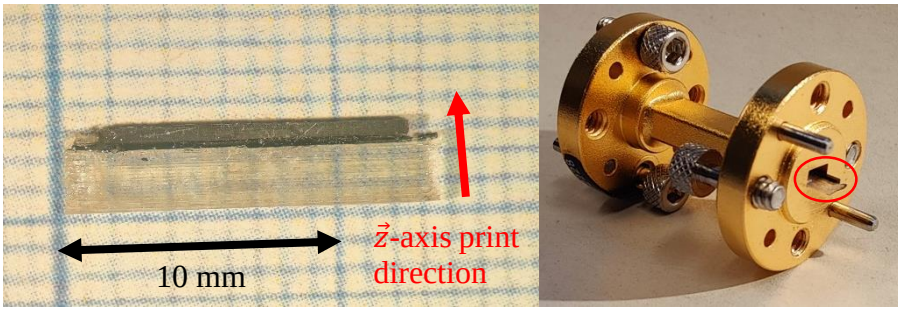

Fig. 5. Detail views of the insert: binocular view (left); insertion into the waveguide (right)

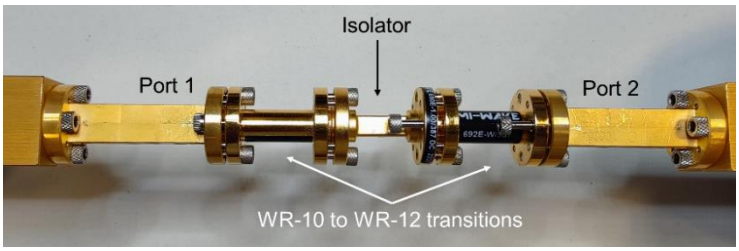

Fig. 6. Measurement setup.

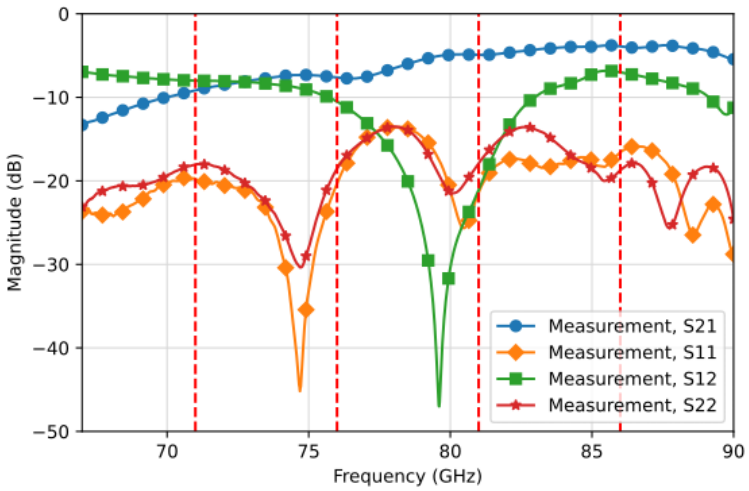

Fig. 7. Measured S-parameters of the realized isolator. Red lines delimit E-band space communication frequency bands (71 – 76 GHz and 81 – 86 GHz).

Simulated and measured RF performances don't match due to multiple reasons. First, some technological variations on the ferrite placement and on the dimensions of 3D printed parts exist. Field-displacement isolators are very sensitive to the position of the ferrite slab that can impact insertion loss.

Second, an inaccurate estimation of material properties can lead to a shift in frequency and/or a variation on the isolation bandwidth. The observed shift in frequency is mainly owing to a wrong estimation of the permittivity value ϵ_r of the ferrite. Commercial hexaferrites shows high values of ϵ_r between 18 and 21 whereas the realized material seems to have a permittivity of 12. It is explained by the density difference [14]. Commercial materials have a density close to 5 g/cm^3 while the Al-doped strontium hexaferrite synthesized here has a density of 4.3 g/cm^3. A longer heat treatment and at a higher temperature can improve its density. It implies a strong shift of the RF response of the isolator towards the high frequencies. Thus, the manufactured isolator is not optimized which leads to a degradation on other characteristics than the central frequency such as insertion loss. Fortunately, this component is closer to the E-band satellite uplink frequency band (81 – 86 GHz).

CONCLUSION

In this paper, an E-band self-biased waveguide isolator has been fabricated and shows fairly good isolation over a wide band ($S_{12} < -12\ dB\ @\ 76.7GHz - 82.3\ GHz$) using the field-displacement effect. It is quite cheap, lightweight, compact and robust to strong magnetic field. Although insertion loss is high ($S_{21} \sim 5\ dB$), this isolator can be used "as-is" in non-demanding applications such as in CubeSats where size, weight and cost are at a premium. With mature industrial manufacturing process, state-of-the-art RF performance can be achieved with Al-doped hexaferrites for E-band or W-band self-biased devices. To get the best RF performance out of these materials, the realized isolator presented above should be re-optimized with the revised ferrite permittivity value of 12. Depending on the final application requirements, the length of the isolator can also be adjusted to reduce insertion loss to the detriment of isolation level.

REFERENCES

[1] F. K. H. Gellersen, C. Diker, J. Peschel, A. Ochsenfarth, and A. F. Jacob, "Doped Barium Hexaferrite Films for Self-Biased Nonreciprocal Components in the Q-/V-Band," *IEEE Antennas Wirel. Propag. Lett.*, vol. 17, no. 11, pp. 1938–1942, Nov. 2018, doi: 10.1109/LAWP.2018.2866547.

[2] E. Roué *et al.*, "Three-Dimensional Printing of a Waveguide Termination for Millimeter Wave Applications," in *2021 51st European Microwave Conference (EuMC)*, Apr. 2022, pp. 555–558. doi: 10.23919/EuMC50147.2022.9784182.

[3] D. Polder, "On the theory of ferromagnetic resonance," *Lond. Edinb. Dublin Philos. Mag. J. Sci.*, vol. 40, no. 300, pp. 99–115, Jan. 1949, doi: 10.1080/14786444908561215.

[4] A. G. Fox, S. E. Miller, and M. T. Weiss, "Behavior and applications of ferrites in the microwave region," *Bell Syst. Tech. J.*, vol. 34, no. 1, pp. 5–103, Jan. 1955, doi: 10.1002/j.1538-7305.1955.tb03763.x.

[5] S. Weisbaum and H. Seidel, "The field displacement isolator," *Bell Syst. Tech. J.*, vol. 35, no. 4, pp. 877–898, Jul. 1956, doi: 10.1002/j.1538-7305.1956.tb03806.x.

[6] M. E. Hines, "Reciprocal and Nonreciprocal Modes of Propagation in Ferrite Stripline and Microstrip Devices," *IEEE Trans. Microw. Theory Tech.*, vol. 19, no. 5, Art. no. 5, May 1971, doi: 10.1109/TMTT.1971.1127545.

[7] D. R. Taft, G. R. Harrison, and L. R. Hodges, "Millimeter Resonance Isolators Utilizing Hexagonal Ferrites," *IEEE Trans. Microw. Theory Tech.*, vol. 11, no. 5, Art. no. 5, Sep. 1963, doi: 10.1109/TMTT.1963.1125674.

[8] J.-L. Mattei *et al.*, "A simple process to obtain anisotropic self-biased magnets constituted of stacked barium ferrite single domain particles," *J. Magn. Magn. Mater.*, vol. 451, pp. 208–213, Apr. 2018, doi: 10.1016/j.jmmm.2017.10.121.

[9] A. Hoez, J.-L. Mattei, and A. Chevalier, "New Manufacturing Process for Granular Texture Management in Polycrystalline BaM Hexaferrites through the Goethite Crystallite Laths Aspect Ratio, and a Specialized Law of Approach to the Magnetic Saturation for Partly Polarized Uniaxial Materials," *Magnetochemistry*, vol. 9, no. 1, Art. no. 1, Jan. 2023, doi: 10.3390/magnetochemistry9010030.

[10] V. Petříček, M. Dušek, and L. Palatinus, "Crystallographic Computing System JANA2006: General features," *Z. Für Krist. - Cryst. Mater.*, vol. 229, no. 5, pp. 345–352, May 2014, doi: 10.1515/zkri-2014-1737.

[11] V. Laur, A. Maalouf, A. Chevalier, and F. Comblet, "Three-Dimensional Printing of Honeycomb Microwave Absorbers: Feasibility and Innovative Multiscale Topologies," *IEEE Trans. Electromagn. Compat.*, pp. 1–8, 2020, doi: 10.1109/TEMC.2020.3006328.

[12] V. Laur, A. Maalouf, A. Chevalier, P. Laurent, and G. Zinkiewicz, "Ultra-compact K-band microwave terminations," in *2022 IEEE Radio and Wireless Symposium (RWS)*, Jan. 2022, pp. 75–78. doi: 10.1109/RWS53089.2022.9719958.

[13] A. Aharoni, "Demagnetizing factors for rectangular ferromagnetic prisms," *J. Appl. Phys.*, vol. 83, no. 6, pp. 3432–3434, Mar. 1998, doi: 10.1063/1.367113.

[14] L. Du *et al.*, "Effect of closed pores on dielectric properties of 0.8Na0.5Bi0.5TiO3-0.2K0.5Bi0.5TiO3 porous ceramics," *J. Eur. Ceram. Soc.*, vol. 38, no. 7, pp. 2767–2773, Jul. 2018, doi: 10.1016/j.jeurceramsoc.2018.02.011.